Polymorphism of $CBrCl_3$

Benjamin Parat,[†] Luis C. Pardo,[†] María Barrio,[†] Josep Ll. Tamarit,*[,†] Philippe Negrier,[‡] Josep Salud,[†] David O. López,[†] and Denise Mondieig[‡]

Laboratory of Characterization of Materials, Department of Physics and Nuclear Engineering, E.T.S.E.I.B., Universitat Politècnica de Catalunya, Diagonal 647, 08028 Barcelona, Catalonia, Spain, and Centre de Physique Moléculaire, Optique et Hertzienne, UMR 5798 au CNRS, Université Bordeaux I, 351, cours de la Libération, 33405 Talence Cedex, France

Received February 18, 2005. Revised Manuscript Received April 12, 2005

The polymorphism of bromotrichloromethane ($CBrCl_3$) has been investigated by X-ray powder diffraction and high-pressure density experiments. Phase transitions as a function of temperature and pressure between the different phases have been characterized at normal pressure as well as at high pressures (up to 300 MPa). From the $p-v-T$ diagram (and the derived $p-T$ diagram) the volume variations at the transition points have been calculated and compared with those obtained by means of X-ray powder diffraction characterization. Special attention is given to the lattice symmetry of the orientational disordered phase II, characterized as rhombohedral ($a = 14.639(8)$ Å, $\alpha = 89.44(1)°$ at 240.2 K). The existence of a glass transition from the monoclinic low-temperature stable ordered phase (III) to its nonergodic state (associated with the freezing of exchange positions between Cl and Br atoms) is analyzed in terms of the asymmetry of the intermolecular interactions, and a new "fingerprint" for the glass transition is proposed on the basis of the aspherism index. Lattice parameters as a function of temperature were determined in order to build up the thermal expansion tensor.

1. Introduction

Molecular crystals are known for their rich polymorphism due to rotational and intramolecular degrees of freedom. Orientationally disordered (or plastic) molecular crystals have been found to be particularly interesting materials due to the existence of many close-packing structures.[1−3] Among them, tetrahalomethanes have been the focus of many studies[4−28] by many workers since the pioneering works of Miller et al.[27,28] on orientational disorder of tetrahedral molecules.

These "simple" molecular compounds are fascinating for two reasons. First, they exhibit a series of thermally induced solid−solid phase transitions before melting that are attributed to the ability to gain rotational degrees of freedom in the crystalline state (orientationally disordered phases, OD) due to the little hindrance for reorientational processes produced by the more or less globular shape of the molecules.[1,2] Second, some of them are well-known monocomponent systems displaying phases with a monotropic character.[4,5,9,10,12−22] The existence of such metastable phases (generally displaying highly symmetrical structures) enables comparison of the interaction potentials with the stable OD phase and thus, to find the fine-tuning producing the stability differences.

Additional reasons making this series of compounds of great interest can be claimed. One of them is that minor changes in the molecular size or in the molecular symmetry can be induced by the change of one of the halogen atoms, giving rise to changes in the intermolecular interactions and,

* To whom correspondence should be addressed. Phone: +34 93 401 65 64. Fax +34 93 401 18 39. E-mail: jose.luis.tamarit@upc.edu.
[†] Universitat Politècnica de Catalunya.
[‡] Université Bordeaux.

(1) Sherwood, J. N. *The Plastically Crystalline (Orientationally-Disordered Crystals)*; Wiley: New York, 1979.
(2) Parsonage, N.; Staveley, L. A. K. *Disorder in Crystals*; Clarendon Press: Oxford, 1978.
(3) Guthrie, G. B.; McCollough, J. P. *J. Phys. Chem. Solids* **1961**, *18*, 53.
(4) Rudman, R.; Post, B. *Mol. Cryst.* **1968**, *5*, 95.
(5) Rudman, R. *Mol. Cryst. Liq. Cryst.* **1970**, *6*, 427.
(6) Rudman, R. *J. Mol. Struct.* **2001**, *569*, 157.
(7) Rudman, R. *J. Chem. Phys.* **1977**, *66*, 3139.
(8) Silver, L.; Rudman, R. *J. Chem. Phys.* **1970**, *74*, 3134.
(9) Struts, A. V.; Bezrukov, O. F. *Chem. Phys. Lett.* **1995**, *232*, 181.
(10) Struts, A. V. *Phys. Rev. B.* **1995**, *51*, 5673.
(11) Akimov, M. N.; Bezrukov, O. F.; Chikunov, O. V.; Struts, A. V. *J. Chem. Phys.* **1991**, *95*, 22.
(12) Pardo, L. C.: Barrio, M.; Tamarit, J. Ll.; López, D. O.; Salud, J.; Negrier, P.; Mondieig, D. *Chem. Phys. Lett.* **1999**, *308*, 204.
(13) Pardo, L. C.: Barrio, M.; Tamarit, J. Ll.; López, D. O.; Salud, J.; Negrier, P.; Mondieig, D. *Chem. Phys. Lett.* **2000**, *321*, 438.
(14) Tamarit, J. Ll.; López, D. O.; Alcobé, X.; Barrio, M.; Salud, J.; Pardo, L. C. *Chem. Mater.* **2000**, *12*, 555.
(15) Pardo, L. C.; Barrio, M.; Tamarit, J. Ll.; López, D. O.; Salud, J.; Negrier, P.; Mondieig, D. *Phys. Chem. Chem. Phys.* **2001**, *3*, 2644.
(16) Pardo, L. C.: Barrio, M.; Tamarit, J. Ll.; Negrier, P.; López, D. O.; Salud, J.; Mondieig, D. *J. Phys. Chem. B.* **2001**, *105*, 10326.
(17) Pardo, L. C.: Barrio, M.; Tamarit, J. Ll.; López, D. O.; Salud, J.; Negrier, P.; Mondieig, D. *Chem. Phys. Lett.* **2002**, *355*, 339.
(18) Pardo, L. C.: Barrio, M.; Tamarit, J. Ll.; López, D. O.; Salud, J.; Negrier, P.; Mondieig, D. *Phys. Chem. Chem. Phys.* **2004**, *6*, 417.
(19) Koga, Y.; Morrison, J. A. *J. Chem. Phys.* **1975**, *62*, 3359.
(20) Arentsen, J. G.; Miltenburg, J. C. *J. Chem. Thermodyn.* **1972**, *4*, 789.
(21) Negrier, Ph.; Pardo, L. C.; Salud, J.; Tamarit, J. Ll.; Barrio, M.; Lopez, D. O.; Würflinger, A.; Mondieig, D. *Chem. Mater.* **2002**, *14*, 1921.
(22) Barrio, M.; Pardo, L. C.; Tamarit, J. Ll.; Negrier, Ph.; Lopez, D. O.; Salud, J.; Mondieig, D. *J. Phys. Chem. B* **2004**, *108*, 11089.
(23) Binbrek, O. S.; Lee-Dadswell, S. E.; Torrie, B. H.; Powell, B. M. *Mol. Phys.* **1999**, *96*, 785.
(24) Binbrek, O. S.; Lee-Dadswell, S. E.; Torrie, B. H.; Powell, B. M. *Physica B* **1998**, *241−243*, 459.
(25) Ohta, T.; Yamamuro, O.; Matsuo, T. *J. Phys. Chem.* **1995**, *99*, 2403.
(26) Negrier, P.; Pardo, L. C.; Salud, J.; Tamarit, J. Ll.; Barrio, M.; Lopez, D. O.; Würflinger, A.; Mondieig, D. *Chem. Mater.* **2002**, *14*, 1921.
(27) Miller, R. C.; Smyth, C. P. *J. Am. Chem. Soc.* **1957**, *79*, 20.
(28) Miller, R. C.; Smyth, C. P. *J. Chem. Phys.* **1956**, *24*, 814.

10.1021/cm050372c CCC: $30.25
Published on Web 05/28/2005

Table 1. Transition Temperatures T_c and Enthalpy (ΔH) and Entropy Changes (ΔS) Derived from DSC Calorimetric Measurements and Adiabatic Calorimetry from Reference 25[a], Volume Changes Determined from X-ray and Neutron Powder Diffraction Measurements (Δv^{XR}) and from High-Pressure $P-v-T$ Measurements (Δv^{HP}), Slope of the Pressure−Temperature Two-Phase Equilibria Derived from the Application of the Clausius−Clapeyron Equation (dT_c/dp^{CC}) and Read from the $P-v-T$ Diagram (dT_c/dp^{exp}) of the $CBrCl_3$ at Normal Pressure

property	Transition			
	$M^S \rightarrow R^S$	$R^S \rightarrow FCC^S$	$FCC^S \rightarrow L^S$	$R^m \rightarrow L^S$
T_c/K	238.1	260.3	267.1	265.7[b] (265.5[e])
	238.19[a]	259.34[a]	267.9[a]	
ΔH/kJ·mol^{-1}	4.58	0.515	2.03	2.55[b]
	4.618[a]	0.527[a]	2.032[a]	
ΔS/J·mol^{-1}·K^{-1}	19.23	1.98	7.61	9.58[b]
	19.40[a]	2.03[a]	7.59[a]	
Δv^{XR} ($p = 0.1$ MPa)/cm^3·mol^{-1}	4.31 ± 0.40[c]	1.41 ± 0.30	2.72	
Δv^{HP} ($p = 0.1$ MPa)/cm^3·mol^{-1}	4.20 ± 0.55	1.41 ± 0.12	2.82 ± 0.14	3.65 ± 0.43
$(dT_c/dp)^{CC}$/K· MPa^{-1}	0.218 (0.224[d])	0.714 (0.696[d])	0.357 (0.370[d])	0.380
$(dT_c/dp)^{exp}$/K·MPa^{-1}	0.217 ± 0.009	0.61 ± 0.04	0.38 ± 0.01	0.35 ± 0.01

[b] Values obtained by extrapolation of the [R + L] equilibrium of the $CBrCl_3 + CCl_4$ two-component system (ref 22). [c] Taking into account the results from Binbrek et al. (ref 23) at low temperature. [d] Using the enthalpy values from ref 25. [e] Extrapolated from the $p-T$ phase diagram.

thus, in the phase sequence, i.e., in the polymorphic behavior. Finally, we must mention the physics of the disorder materials and, especially, the challenging problem of understanding the molecular dynamics when the glass transition is approaching, which is, at present, the focus of many experimental investigations.[29−31] For the tetrahalomethanes with T_d molecular symmetry, a high number of experimental and molecular dynamics simulation studies have been published,[32−38] while for the compounds with lower symmetry (C_{3v} or C_{2v}) only a few preliminary experiments have been done.[14,26,33]

The polymorphism of $CBrCl_3$ (C_{3v} molecular symmetry) has been studied earlier by several methods such as calorimetry,[25] neutron scattering,[23,24] densitometry,[39] infrared and Raman spectroscopy,[40] and dielectric spectroscopy.[27,28]

As far as the stable phases are concerned, the thermodynamic properties of the polymorphic behavior of $CBrCl_3$ have been recently stated by means of adiabatic calorimetry from 5 to 300 K[25] and can be described as follows. The low-temperature phase III transforms at 238 K to the OD phase II. On further heating, OD phase I appears at 259 K. Finally, the melting temperature is found at 267 K (enthalpy changes are collected in Table 1). All these transitions were found to be reversible.

The crystal structures of the ordered and OD phases of $CBrCl_3$ were attempted by Binbrek et al.[23] They described the structure of the phase III of $CBrCl_3$, from neutron powder diffraction, in terms of the $C2/c$ space group with $Z = 32$, on the basis of the hypothesis of the isostructural character of the low-temperature ordered phases for all four members of the CCl_nBr_{4-n} ($n = 0,...,4$) family. For this *ordered* phase III of the $CBrCl_3$ compound the molecules were assumed to be disordered so that sites have fractional occupancies of 0.75 and 0.25 for each of Cl and Br atoms, respectively. The authors also identified the unit cell of the high-temperature OD FCC,[23,24] but attempts to determine the lattice symmetry of the intermediate OD phase II were unsuccessful.

One of the reasons to delve into the study of these materials is that, because of the presence of competing interactions, these show a number of "glassy features" that can be studied on these simple systems. In particular $CBrCl_3$ undergoes a glass transition at about 90 K associated with the freezing of exchange positions between Cl and Br atoms.[25] The existence of such a glass transition means that below 90 K the system is not in an equilibrium state and thus, that the transition to a plausible additional phase at a lower temperature, in which the Cl and Br atoms occupy defined site positions, is missing.

The present work is the first comprehensive study of the polymorphism of $CBrCl_3$ as a function of pressure and temperature. This paper is organized as follows. Section 2 describes the experimental techniques and procedures. Section 3 reviews the thermodynamic and crystallographic properties of $CBrCl_3$ determined in this work. Section 4 summarizes the results, and Section 5 is devoted to the conclusions.

2. Experimental Section

2.1 Samples. $CBrCl_3$ with purity higher than 99% was purchased from Aldrich and was used without further purification.

2.2 Equipment. *X-ray Diffraction.* X-ray diffraction patterns were recorded using a horizontally mounted INEL cylindrical position-sensitive detector (CPS120)[41] equipped with a liquid nitrogen 600 series Cryostream Cooler from Oxford Cryosystems. The detector, used in Debye−Scherrer geometry (transmission mode), consisted of 4096 channels and enabled a simultaneous recording of the profile over a 2θ range between 4 and 120° (angular step of 0.029° in 2θ). Monochromatic Cu $K\alpha_1$ ($\lambda = 1.54059$ Å)

(29) Lunkenheimer, P.; Schneider, U.; Brand, R.; Loidl, A. *Contemp. Phys.* **2000**, *41*, 15.
(30) Höchli, U. T.; Knorr, K.; Loidl, A. *Adv. Phys.* **1990**, *39*, 405.
(31) Angell, C. A.; Ngai, K. L.; McKenna, G. B.; McMillan, P. F.; Martin, S. W. *J. Appl. Phys.* **2000**, *88*, 3113.
(32) Narten, A. H. *J. Chem. Phys.* **1979**, *70*, 299.
(33) Rey, R.; Pardo, L. C.; Llanta, E.; Ando, K.; López, D. O.; Tamarit J. Ll.; Barrio, M.; *J. Chem. Phys.* **2000**, *112*, 7505.
(34) Llanta, E.; Rey, R. *Chem. Phys. Lett.* **2001**, *340*, 173.
(35) Bermejo, F. J.; Enciso, E.; Alonso, J.; Garcia, N.; Howells, W. S. *Mol. Phys.* **1988**, *64*, 1169.
(36) Egelstaff, P. A.; Page, D. I.; Powles, J. G. *Mol. Phys.* **1971**, *20*, 881.
(37) Lowden, L. J.; Chandler, D. *J. Chem. Phys*. **1974**, *61*, 5228.
(38) Jóvári, P.; György, M.; Pusztai, L.; Sváb, E. *J. Chem. Phys.* **2001**, *114*, 8082.
(39) Jarne, C.; Artal, M.; Muñoz-Embid, J.; Velasco, I.; Otín, S. *Can. J. Chem.* **1999**, *77*, 2046.
(40) Park, Y. S.; Shurvell, H. F. *Can. J. Spectrosc.* **1988**, *33* (2), 38.
(41) Ballon, J.; Comparat, V.; Pouxe, J. *Nucl. Instrum. Methods* **1983**, *217*, 213.

radiation was selected by means of an asymmetric focusing incident-beam curved quartz monochromator. The generator power was set to 1.0 kW (40 kV and 25 mA).

The sample was introduced into 0.3-mm-diameter Lindemann glass capillaries in the liquid state at room temperature and was rotated perpendicularly to the X-ray beam during data collection to improve averaging of the crystallites.

Patterns were obtained on heating every 10 K in the temperature range of 175−235 K and every 5 K from this temperature up to the melting point, with acquisition times of at least 60 min and a stabilization time of at least 10 min at each temperature before the data acquisition.

External calibration by means of cubic phase $Na_2Ca_3Al_2F_{14}$ was performed for channels to be converted into 2θ degrees by means of cubic spline fittings.[42] PEAKOC application from DIFFRACTINEL software was used for the calibration and for the peak position determinations after pseudo-Voigt fittings. Lattice parameters were refined by means of the FullProf program.[43]

Density. Measurements at normal pressure in the liquid state from 278 to 353 K were carried out using an Anton Paar D5000 densimeter with temperature stability of ±0.02 K, giving rise to uncertainties in density of ca. 5×10^{-5} g·cm^{-3}. The densimeter was calibrated with bidistilled water and *n*-hexane (99.9%). The density values were taken from references.[44,45]

High-pressure density values were determined by means of a homemade pvT apparatus (uncertainty of ca. 10^{-4} g·cm^{-3}) from the high-pressure laboratory of Prof. Dr. A. Würflinger (Ruhr-Universität, Bochum, Germany). Details of the experimental system and the procedure have been reported elsewhere.[46]

Calorimetry. Temperature and enthalpy change of the phase transitions were measured using a Perkin-Elmer DSC-7 differential scanning calorimeter equipped with a low-temperature system.

3. Results

Temperature and enthalpy changes at the solid−solid and melting transitions determined by means of calorimetry are summarized in Table 1. It can be seen that results match up with those previously determined from adiabatic calorimetry,[25] within the experimental error.

X-ray powder diffraction experiments were conducted from 175 K up to the liquid state. Patterns of the low-temperature monoclinic phase III were submitted to Rietveld profile refinement by means of the "pattern-matching" option of the FullProf program and on the basis of the structure proposed by Binbrek et al.[23] It is noteworthy that the structural parameters of CBr_4[47] were used as the starting point for the atomic coordinates of the four molecules in the asymmetric unit; the fractional occupancies of the halogen sites were set as 0.25 and 0.75 for Br and Cl atoms, respectively, and rigid body representing a pseudo-molecule with tetrahedral symmetry in which overlapping Br and Cl atoms located at 1.939 and 1.772 Å from the central carbon atom C (slightly different from those used initially in the work of Binbrek et al.[23]), respectively, was used. Figure 1 shows the experimental and calculated profiles together with the difference between them. The monoclinic lattice parameters of $CBrCl_3$ agree quite well with those previously published.[23] At 223.2 K they have been determined to be $a = 20.620(5)$ Å, $b = 11.613(3)$ Å, $c = 20.195(5)$ Å, and $\beta = 111.223(6)°$. Figure 2A shows the agreement between the lattice parameters determined in this work and those determined from neutron scattering.[23]

As far as phase II is concerned, it has been recently demonstrated[22] that this phase and phase Ib of CCl_4 (the symmetry of which is rhombohedral) are related by an

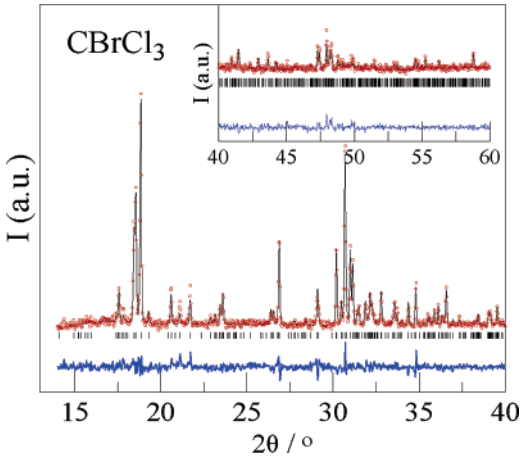

Figure 1. Experimental (○) and theoretical (−) diffraction patterns of phase III (*C*2/*c*) for $CBrCl_3$ at $T = 223.2$ K along with the difference profile (lower curve). The intensity of the inset is magnified 4 times.

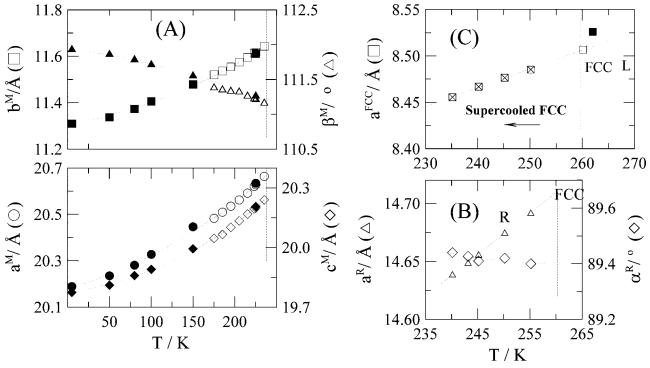

Figure 2. Lattice parameters of $CBrCl_3$ for phases III (A), II (B), and I (C) as a function of temperature. Full symbols correspond to refs 23 and 24. Crossed squares correspond to the supercooled phase I.

Table 2. Experimental (d_{obs}) and Calculated (d_{cal}) Lattice Spacings (in Å) for the Reflections *hkl* of the OD Rhombohedral Stable Phase of CCl_3Br Compound at 240.2 K ($a = 14.639(8)$ Å, $\alpha = 89.44(1)°$)

h k l	d_{obs} (Å)	d_{cal} (Å)	$d_{obs} - d_{cal}$ (Å)
−2 2 0	5.1471	5.1502	−0.0031
2 2 1	4.9195	4.9218	−0.0023
3 0 0	4.8739	4.8792	−0.0053
2−2 1	4.8519	4.8583	−0.0063
3 1 0	4.6408	4.6423	−0.0015
3−1 0	4.6123	4.6154	−0.0031
3 1 1	4.4426	4.4409	0.0017
3−1 1	4.4109	4.4095	0.0014
3 1 2	3.9413	3.9422	−0.0009
2−1 3	3.9165	3.9147	0.0018
1−3 2	3.8953	3.8932	0.0021
4 1 3	2.8921	2.8912	0.0009
1−4 3	2.8584	2.8568	0.0016

(42) Evain, M.; Deniard, P.; Jouanneaux, A.; Brec, R. *J. Appl. Crystallogr.* **1993**, *26*, 563.
(43) Rodriguez-Carvajal, J.; Roisnel, T.; Gonzales-Platas, J. FullProf Suite (April 2004 version); Laboratoire Léon Brillouin, CEA-CNRS, CEN Saclay, France.
(44) Randzio, S. L.; Grolier, J.-P. E.; Quint, J. R.; Eatough, D. J.; Lewis, E. A.; Hansen, L. D. *Int. J. Thermophys.* **1994**, *15*, 415.
(45) Mopsik, F. I. *J. Res. Nat. Bur. Stand. Sec. A* **1967**, *71*, 287.
(46) Würflinger, A.; Sandmann, M.; Weissflog, W. *Z. Naturforsch.* **2000**, *55a*, 823.
(47) More, M.; Baert, F.; Lefebvre, J. *Acta Crystallogr.* **1977**, *B33*, 3681.

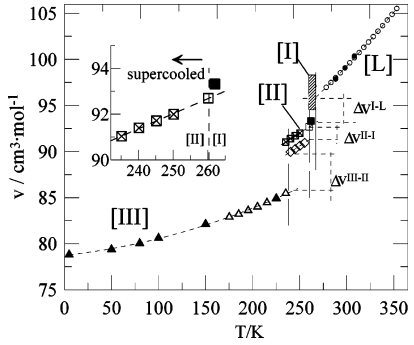

Figure 3. Molar volume of $CBrCl_3$ as a function of temperature at normal pressure. Full symbols for solid phases (▲, phase III; ■, phase I) were obtained from refs 23 and 24, and for liquid phase (●) were obtained from ref 39. Dashed region corresponds to the stability domain of phase I. Inset magnifies the molar volume (crossed squares) of the supercooled phase I.

isomorphism relationship. On the basis of this result, experimental pattern of phase II at 240.2 K was submitted to a lattice parameter refinement using the pattern-matching option (see Table 2). Subsequently, lattice parameters were refined at each temperature (Figure 2B).

Patterns as a function of temperature were also collected for phase I and, due to the narrow temperature domain of existence, measurements were extended to lower temperatures by supercooling the phase down to 235 K. As can be seen in Figure 2C there is a close agreement between the trends of the values of the present work and the corresponding value previously reported.[24]

From the lattice parameters as a function of temperature, molar volume was calculated and, together with the density measurements for the liquid phase, the volume changes at the phase transitions (at normal pressure) could be determined (Figure 3).

High-pressure density measurements were undertaken up to 300 MPa for a representative number of isotherms (see Figure 4). From the pressure transition at each measured temperature, the pressure−temperature phase diagram has been built up and it is shown in the inset of Figure 4.

The inset in Figure 4 points out the existence of a triple point (31 MPa, 278.7 K) sharing the liquid and the R and FCC OD phases, which implies the disappearance of the OD FCC phase at high pressures.

4. Discussion

Recently, the stable and metastable melting parts of the $CBrCl_3 + CCl_4$ phase diagram have been determined (Figure 5).[22] As a consequence of the monotropic behavior of the FCC melting for a large concentration domain, the [FCC + L] metastable equilibrium could be experimentally determined from $X = 0$ (CCl_4) up to the peritectic point, being the thermodynamic analysis of the complete [FCC + L] equilibrium the demonstration of the coherence between the stable and the metastable parts as a whole. The extrapolation at $X = 1$ of the stable [R + L] equilibrium enables determination of the metastable (and experimentally nonavailable) melting temperature of the R phase of the $CBrCl_3$ compound at normal pressure, which is found to be 265.7 K. Such a temperature should be understood as the temperature at which the R phase would melt (at normal pressure) if the FCC phase would not exist. This result can be now compared with the extrapolation of the R melting curve as a function of pressure (see $p-T$ phase diagram, inset of Figure 4) to normal pressure. By so doing, the resulting melting temperature of the phase R of $CBrCl_3$ at normal pressure is 265.5 K, which clearly agrees within the experimental error limits.

From Figure 4, volume changes for the different phase transitions as a function of pressure can be determined (Figure 6). Such results can be extrapolated at normal pressure (see dashed curves in Figure 6) and compared with those obtained at normal pressure from X-ray diffraction and density values. It can be seen that there is good agreement for the measured transitions. In addition, the volume change for the metastable melting of the R phase at normal pressure is well defined. To address the question whether ΔV^{R-L} has a reasonable physical value, it has been replaced into the Clausius−Clapeyron equation (dT_c/dp^{CC}) and, together with the enthalpy change obtained from the extrapolation of the enthalpy data as a function of composition for the $CBrCl_3 + CCl_4$ phase diagram,[22] compared with the experimental slope ($(dT_c/dp)^{exp}$) obtained at pressures higher than ca. 30 MPa. Both sets of values are summarized in Table 1 and the agreement is comparable to the other phase transitions for which the whole set of values are experimentally available.

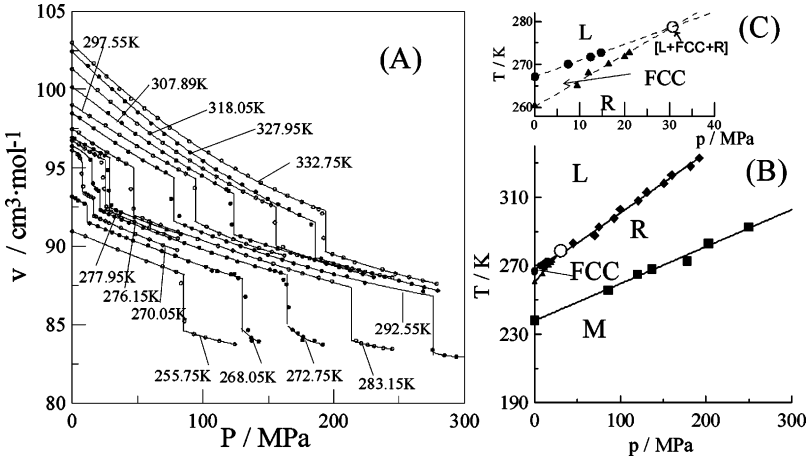

Figure 4. Molar volume as a function of pressure for several temperatures (A). Pressure−temperature phase diagram for $CBrCl_3$ (B), and a detail of the low-pressure region (C).

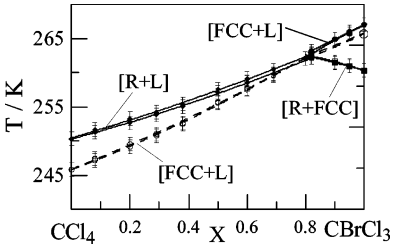

Figure 5. Stable (continuous line) and metastable (dashed line) $CBrCl_3 + CCl_4$ melting phase diagrams from ref 22. The dashed lines show the experimental [FCC + L] equilibrium (from X = 0 to X ≈ 0.8) and the extrapolation of the [R + L] equilibrium at X = 1, giving rise to the hypothetical melting temperature (at 265.7 K, ○) of the R phase of $CBrCl_3$.

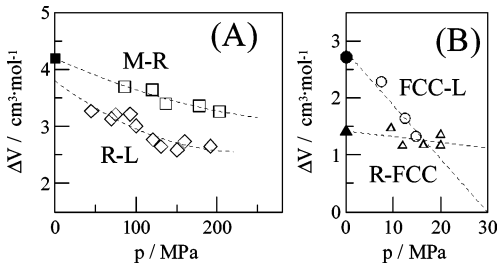

Figure 6. (A) Volume changes as a function of pressure for the phase transitions M−R (□) and R−L (◇), and (B) R−FCC (△) and FCC−L (○) of $CBrCl_3$ derived from $p\nu T$ measurements (empty symbols) and from X-ray and liquid density measurements at normal pressure (filled symbols).

Two interesting experimental results can be determined from Figure 6. First, the M − R and R − L volume changes seem to stabilize on increasing pressure, which are physically coherent results assuming that these two-phase equilibria do not split and thus any additional solid phase appears in the measured pressure range. Second, the FCC − L volume change diminishes with pressure and becomes zero at around 30 MPa, which is virtually the same pressure as that of the R + FCC + L triple point of the $p-T$ diagram.

The anisotropy of the intermolecular interactions in the solid state has been studied by means of the analysis of the isobaric thermal expansion tensor. The cell deformation dU due to a small temperature variation dT is expressed by a second-rank tensor $dU_{ij} = \alpha_{ij}\, dT$, where α_{ij} (K^{-1}) are the coefficients of the thermal expansion tensor. At a given temperature, the knowledge of the principal coefficients and of the direction of the principal axes of the tensor allows the determination of the strongest and the weakest directions of the corresponding intermolecular interactions, commonly referred to as "hard" and "soft" directions, respectively.[48]

The lattice parameters were fitted as a function of the temperature using a standard least-squares method. The agreement between the calculated and experimental values has been accounted by the reliability factor, defined as $R^2 = \sum[y_o - y_C]^2/y_C^2$, where y_o and y_C are the measured and calculated lattice parameters, respectively.

For a monoclinic lattice the tensor is completely defined by the principal coefficients, α_1, α_2, and α_3, and an angle Φ between the direction of one of the principal directions (α_3 in the present case) and the crystallographic axis ***a***, the α_2 axis being coincident with the 2-fold axis ***b*** of the crystal. For phase III, lattice parameters from neutron diffraction as well as from X-ray diffraction were used in the temperature-fitting procedure. The parameters of the fitting, given in Table 3, are in good agreement within the limit of experimental error.

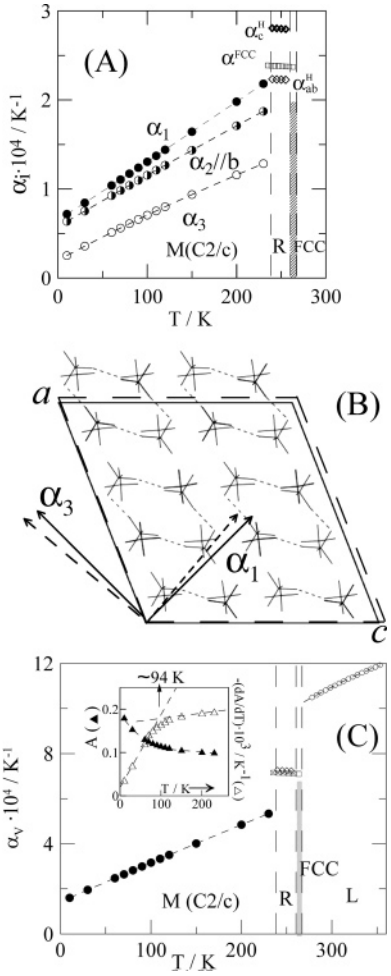

Figure 7. (A) The α_i principal coefficients as a function of temperature for $CBrCl_3$: circles, monoclinic phase III (α_2 is chosen parallel to the crystallographic direction **b** in the monoclinic phase); rhombus, rhombohedral phase II in the hexagonal setting; and squares, FCC phase I (supercooled domain is enclosed). For T < 90 K, values correspond to the glassy state of phase III. (B) Projections of the monoclinic structure of phase III of $CBrCl_3$ (dashed line) and axes of phase II of CCl_4 (continuous line) on the (0*k*0) crystallographic plane. Dashed lines between molecules correspond to the shortest distances. (C) The volume expansivity (α_v) as a function of temperature. As an inset, the aspherism index (*A*) and its derivative (d*A*/d*T*) as a function of the temperature for phase III are shown. Dashed areas correspond to the stability domain of the OD FCC phase, although lattice parameters and thus, the thermal-expansion tensor, were determined on cooling to around 235 K.

Figure 7A depicts the variation of the principal coefficients of the thermal expansion tensor as a function of temperature. In the whole studied temperature range of phase III the α_3 direction corresponds to the hardest direction, as can be also seen in Figure 8A, where a three-dimensional plot of the isobaric thermal expansion tensor for this phase is presented. It should be noticed that the structural model imposes a dynamic disorder involving the exchange of Cl and Br atoms on fixed sites making it impossible to define the orientation of the molecular dipole and, thus, a more detailed correlation between the interactions and the structure.

Nevertheless, on the basis of the model, some comparisons with the CCl_4 and CBr_4 low-temperature structures can be

(48) Salud, J.; Barrio, M.; López, D. O.; Tamarit, J. Ll.; Alcobé, X. *J. Appl. Crystallogr.* **1998**, *31*, 748.

Table 3. Polynomial Equations $P = p_o + p_1T + p_2T^2$ (T in K and p in Å or in deg for β Parameter) to Which the Lattice Parameters Were Fitted as a Function of Temperature; R Is the Reliability Factor

phase	temperature range (K)	parameter	p_o	$p_1 \times 10^3$	$p_2 \times 10^5$	$R \times 10^4$
III	5−235	a/Å	20.181(8)	0.953(4)	0.46(5)	3.6
		b/Å	11.302(4)	0.65(7)	0.33(2)	3.0
		c/Å	19.775(6)	0.471(11)	0.63(4)	2.8
		β/deg	111.96(3)	−2.0(5)	−0.57(20)	2.3
II	240−255	a_H/Å	19.49(6)	4.6(2)		2.2
		c_H/Å	25.88(9)	7.2(4)		2.3
I	235−267	a/Å	7.98(1)	2.02(4)		1.7

done. For these CX_4 compounds (and thus for the $CBrCl_3$ structural model) it was shown that C−X distances and X−C−X angles fall, within the experimental error, in the values expected for a regular tetrahedron.[47,49] For $CBrCl_3$, although it seems to be rather unlikely that the assumed tetrahedral symmetry holds, due to the asymmetry in size and interatomic distances of the halogen atoms, the disorder involving such halogen atoms provides (as the results shown) a quite similar structure. In this context, Figure 7B shows the CCl_4 unit cell projected along [010] together with the unit cell of the $CBrCl_3$ as well as the principal directions α_1 and α_3 for both structures. It can be seen that the shortest distances (dashed lines in Figure 7B) lie on this plane and that principal directions for both thermal expansion tensors are virtually the same.

One experimental result which must be taken as evidence of the tetrahedral imposed molecular symmetry is the shortest Br···Br intermolecular distance, which is found to be 3.521−3.567 Å. Such a distance is between the Cl···Cl (2.889 Å)[49] and Br···Br (3.776 Å)[47] found for CCl_4 and CBr_4, respectively, for which chlorine and bromine atoms of each molecule are certainly located at the corners of a regular tetrahedron.

To make evident the anisotropy of the thermal expansion tensor in the orientationally disordered phase II, the rhombohedral lattice has been described in terms of a hexagonal setting ($a_H = 2a_R\sin(\alpha_R/2)$; $c_H = a_R[3(1 + 2\cos\alpha_R)]^{1/2}$). According to the Newmann principle, for which the thermal-expansion tensor has to display the point group symmetries of the crystal, the 3-fold hexagonal axis c must be a revolution axis of the tensor. In this way the principal directions and thus, the principal coefficients, are reduced to two independent directions: α_c, parallel to the $\boldsymbol{c}$ crystallographic direction, and α_{ab}, which accounts for the thermal expansion in any direction of the (00l) plane (Figure 7A). Figure 8B displays the three-dimensional plot of the tensor for this phase. Note that the thermal-expansion along the 3-fold hexagonal axis $\boldsymbol{c}$ is greater than in the (00l) plane, a feature completely equivalent to the previous scheme determined for the $(CH_3)_2CCl_2$ methylchloromethane.[26] Moreover, the principal coefficient of the FCC OD phase is determined to be between the α_c and the α_{ab} values of the phase II, as it was for the mentioned $(CH_3)_2CCl_2$ and as it was expected because of the close similarity between these OD high-temperature phases.

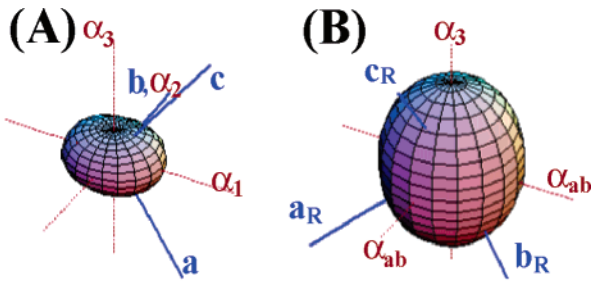

Figure 8. Thermal-expansion tensors of phases III of $CBrCl_3$ at T =150 K (A) and II at T =250 K (B) in the frame of the principal directions α_i (dotted red lines) together with the crystallographic axes (continuous blue lines). The full length of the α_i axes corresponds to 8×0^{-4} K^{-1}.

The volume expansivity α_V (equal to $\alpha_1 + \alpha_2 + \alpha_3$) is depicted in Figure 7C as a function of temperature for solid and liquid phases. The lowest volume expansivity corresponds to phase III as a consequence of the higher intermolecular interactions. It should be noted that, beyond what is expected from ordinary anharmonic effects, no changes in the slopes of the lattice parameters versus temperature (Figure 2), as expected for a glass transition, could be found. The glass transition leading from monoclinic ergodic phase III to the glass state (at $T < T_g$) should be understood as a purely dynamic crossover, because of the presence of long-range positional periodicity at both sides of the glass transition at which exchanges of the Cl and Br atoms freeze. For both the canonical glass transition (obtained by supercooling a liquid phase) and the common orientational glasses obtained from supercooling an orientational disordered (plastic) phase, temperature of glass transition must be signaled by a jump in thermal expansivity (Figure 7C). In the present case, the anomaly might be too small to be observed. Thus, the detection of the anomaly was only possible owing to the numerical derivative analysis of the aspherism coefficient.[50] This coefficient enhances the details of the intermolecular interaction anisotropy, and is defined as:

$$A = (^2/_3)[1 - (3\beta/\alpha_v^2)]^{(1/2)}$$

where $\beta = \alpha_1\alpha_2 + \alpha_2\alpha_3 + \alpha_1\alpha_3$. The aspherism index of the monoclinic phase slowly decreases with temperature, experimental evidence of the increase of the isotropy of the intermolecular interactions. In addition, it can be noted that at ca. 94 K there is a change in the variation of the aspherism index as a function of the temperature. The question arises whether such a change can be considered as a signature of the glass transition, at which the dynamics from the nonergodic to the ergodic states should produce a change in the intermolecular interaction potential.

5. Conclusions

The use of different techniques, as well as basic thermodynamics, has not only provided information about the stable

(49) Cohen, S.; Powers, R.; Rudman, R. *Acta Crystallogr.* **1979**, *B35*, 1670.
(50) Weigel, D.; Beguemsi, T.; Garnier, P.; Gerad J. F. *J. Solid State Chem.* **1978**, *23*, 241.

experimentally available phases but has also touched on the nonexperimentally available properties and transitions of metastable phases. In this way, by combining the high-pressure with the normal-pressure experimental data, the temperature, entropy, and volume variations for the melting of the R phase at normal pressure have been determined. The thermodynamic high-pressure data evidence the existence of a triple point [R + FCC + L] in such a way that only the OD R phase remains stable at high pressure ($p \geq$ 31 MPa).

As for the lattice symmetry, results obtained for the monoclinic phase III ($C2/c$) match up perfectly with those previously reported by Binbrek et al.[23] The lattice symmetry of the OD phase II (rhombohedral) has been also established. Although both results are obtained from X-ray powder diffraction (or neutron powder diffraction in ref 23) it should be emphasized that volume variations at normal pressure between the different phases as obtained from these crystallographic data, agree quite well according to the experimental error limits with those obtained from density measurements at high-pressure. Such coherence gives credibility to the whole measured quantities.

The analysis of the thermal-expansion tensor has provided the anisotropies of the intermolecular interactions for the studied phases. As for the monoclinic low-temperature phase III, the variation of the lattice parameters as a function of the temperature do not evidence any anomaly at the glass transition. Consequently, the volume of the lattice varies continuously with the temperature and then, the jump of the thermal expansivity is missed according with the measurements performed. Nevertheless, the aspherism index, which accounts for the anisotropy of the intermolecular interactions, shows a change, evidenced by means of its derivative vs temperature, at a temperature close to the calorimetric glass transition.

As far as the orientationally disordered phases are concerned, despite the disorder, the existence of weak interactions along the ***c*** axis of the hexagonal setting of the OD rhombohedral phase II has been evidenced. Moreover, close similarity between OD phases II (R) and I (FCC) is found when physical properties which do not account for the anisotropic properties, such as volume expansivity, are analyzed.

Acknowledgment. We thank the Institute of Physical Chemistry II, Ruhr University (Bochum) for providing the high-pressure pvT device and I. van den Bruwane to perform the calibration of the system. This work was supported by the Spanish Ministry of Science and Technology (BFM2002-01425) and by the Catalan government (SGR2002-00152).

CM050372C